Desalination and Water Treatment
www.deswater.com

doi: 10.1080/19443994.2014.954146

56 (2015) 1829–1838
November

Taylor & Francis
Taylor & Francis Group

Adsorption of As(V) on aluminum-, iron-, and manganese-(oxyhydr)oxides: equilibrium and kinetics

Feihu Li[1,*], Di Geng[2], Qing Cao[3]

Jiangsu Key Lab of Atmospheric Environment Monitoring and Pollution Control, Jiangsu Engineering Technology Center for Environmental Purification Materials Research, School of Environmental Science and Engineering, Nanjing University of Information Science and Technology, Nanjing 210044, China, Tel./Fax: +86 25 5873 1090; email: fhli@nuist.edu.cn (F. Li), Tel. +86 10 6233 3603; email: bjwendy0516@126.com (D. Geng), Tel. +86 853 325 3378; email: oplkpp11@qq.com (Q. Cao)

Received 27 December 2013; Accepted 7 August 2014

ABSTRACT

In the present work, three metal (oxyhydr)oxides, i.e. 2-line ferrihydrite (FeOOH), bayerite (β-Al(OH)$_3$), and hausmannite (Mn_3O_4), were prepared and then employed as adsorbents for As(V) in aqueous solution. Both adsorption equilibrium and kinetics of As(V) have been investigated via batch experiments. The adsorption equilibrium results indicated that all adsorption data follow the Langmuir equation with maximum adsorption capacities of 28.57, 14.29, and 1.00 mg g^{-1} for FeOOH, β-Al(OH)$_3$, and Mn_3O_4, respectively. It was found that the pseudo-second-order kinetic equation is capable of fitting these kinetic data well with correlation coefficients (R^2) greater than 0.98. The effects of co-occurring anions, both phosphate (PO_4^{3-}) and sulfate (SO_4^{2-}), were shown to reduce As(V) uptake, whereas calcium ion (Ca^{2+}) was found to enhance As(V) adsorption. This work can extend our understanding of equilibrium and kinetic behaviors of As(V) adsorption on typical metal (oxyhydr)oxides.

Keywords: Arsenic; Adsorption; Ferrihydrite; Bayerite; Hausmannite; Kinetics

1. Introduction

The mobility, reactivity, bioavailability, and toxicity of trace inorganic contaminants, such as arsenic, in the natural aqueous systems are closely correlated to the sediments consisted of various metal (oxyhydr)oxides [1–4]. Arsenic uptake by various adsorbents has been extensively studied over the last several decades [5–10]. Of these adsorbents, metal (oxyhydr)oxides including iron-[1,3,11–14], aluminum-[15–18], and manganese-[19–21] (oxyhydr)oxides have attracted much attention because of their specific affinity to arsenic. Iron- and aluminum-(oxy)hydroxides were found to be very efficient in the uptake of As(V) [22].

---

[*] Corresponding author.

[1] Present address: Earth Sciences Division, Lawrence Berkeley National Laboratory, One Cyclotron Road, Berkeley, CA 94720, USA

[2] Present address: School of Civil and Environmental Engineering, University of Science and Technology Beijing, Beijing 100083, China

[3] Present address: Anshun Meteorological Bureau, Anshun, Guizhou 561000, China

It was also reported that manganese oxide can effectively oxidize As(III) to As(V) and then sequester As(V) by adsorption [23,24].

Among these studies, some conflicting results regarding either adsorption equilibrium or kinetics are confusing. For example, Pierce and Moore [1] studied the adsorption isotherms of arsenic on amorphous iron hydroxides and found that these adsorption isotherms obeyed the Langmuir model at low initial arsenic concentrations, but followed linear equation at high concentrations. It was also reported that the equilibrium adsorption of As(V) on ferrihydrite complied with the Langmuir equation at pH 4.6, but followed the Freundlich equation at pH 9.2 [25]. Additionally, there has been a lot of debate on As(V) adsorption kinetic models on metal oxyhydroxides. For instance, it is reported that the kinetic data of As(V) adsorption on ferrihydrite followed the pore-space diffusion model [11]. It is also, however, found that the kinetic data of As(V) adsorption on ferrihydrite agreed with the parabolic diffusion model [25]. On the other hand, direct comparison of As(V) adsorption on iron-, aluminum-, and manganese-(oxyhydr)oxides under the same condition is necessary, especially the adsorption equilibrium and kinetic properties, to clarify the above-mentioned contradictions in previous studies. However, litter information on this can be found in the literature. It is, therefore, obliged to re-evaluate both the equilibrium and the kinetics of As(V) adsorption on metal (oxyhydr)oxides.

Here, As(V) adsorption equilibrium, as well as kinetics of iron-, aluminum-, and manganese-(oxyhydr)oxides, has been investigated via batch experiments. The equilibrium data were fitted with both the Langmuir and the Freundlich equations. A versatile kinetic model, namely the pseudo-second-order rate model was employed to fit the kinetic data. In addition, the effects of pH and co-occurring species, such as phosphate, sulfate, and calcium ion on As(V) adsorption, were also evaluated. The findings in this work can extend our understanding in equilibrium as well as the kinetic behaviors of As(V) adsorption on metal (oxyhydr)oxides.

2. Materials and methods

2.1. Chemicals

ACS-grade sodium arsenate dibasic heptahydrate ($Na_2HAsO_4{\cdot}7H_2O$) was purchased from Sigma-Aldrich and used as received. All other reagents (analytical grade) were obtained from Sinopharm Chemical Reagent Co., Ltd, and used without any further purification. Water used was double-deionized water (DD H_2O) passed through a MILLI-Q system.

2.2. Synthesis and characterization of metal (oxyhydr) oxides

Iron oxyhydroxide was prepared following the method from literature [26] with minor changes. Briefly, NaOH (0.2 M) was added to a solution of Fe $(NO_3){\cdot}9H_2O$ (0.375 M) using a peristaltic pump in air at 298 ± 1 K. The reaction was interrupted until the desired experimental pH (e.g. 8.0) was attained. The resultant suspensions were sealed and further aged for 16 h at 298 ± 1 K prior to washing with DD H_2O for at least 10 times, followed by filtration and drying at 313 K for 4 h. Aluminum hydroxide was synthesized following the same procedure as described above. Manganese oxide was prepared by addition of concentrated H_2O_2 (1 mL) to 0.06 M $MnSO_4{\cdot}H_2O$ (20 mL) prior to further addition of 0.2 M NH_4OH (6 mL). The suspension was magnetically stirred before aging at 368 K for 6 h, followed by cooling to room temperature, washing with DD H_2O for 10 times, filtration, and drying at 313 K for 4 h. All synthetic materials were ground and passed 100-mesh sieve prior to use.

X-ray diffraction (XRD) analysis was conducted using a SHIMADZU XRD-6100 diffractmeter at a voltage of 40 kV and a current of 30 mA with Cu-Kα radiation, and the XRD patterns were presented in Fig. 1 The zeta potential (ζ) profiles of the adsorbents measured at 298 K using a Zeta Meter (Zetasizer Nano ZS90, Malvern) and the results were shown in Fig. 2. The zeta potential analysis procedure was depicted elsewhere [27] with a replacement of 0.01 M NaCl solution with 0.1 M NaCl ion-strength solution.

2.3. Adsorption tests

As(V) stock solutions (1,000 mg L^{-1}, eq. 3.21 mM As(V)) were prepared using ACS-grade $Na_2HAsO_4{\cdot}7H_2O$ and diluted as needed. All adsorption tests were done at 298 ± 1 K with a dose of 1 g L^{-1} unless otherwise specified. Adsorption envelopes of As(V) were obtained in 0.1 M NaCl via batch experiments. The initial pH values of individual suspensions were adjusted to certain values in the range of 3–11 using dilute HCl and NaOH, and all suspensions were allowed to react for 24 h on a reciprocating shaker before filtration with 0.45 μm membrane and then analysis of As(V). Adsorption equilibrium experiments were conducted following the same batch experiment procedure as depicted in our previous study [13]. Adsorption kinetic tests were implemented using the procedure described elsewhere [27]. Effects of co-occurring anions (e.g. SO_4^{2-}, PO_4^{3-}) and counterion (e.g. Ca^{2+}) on As(V) uptake were explored by addition

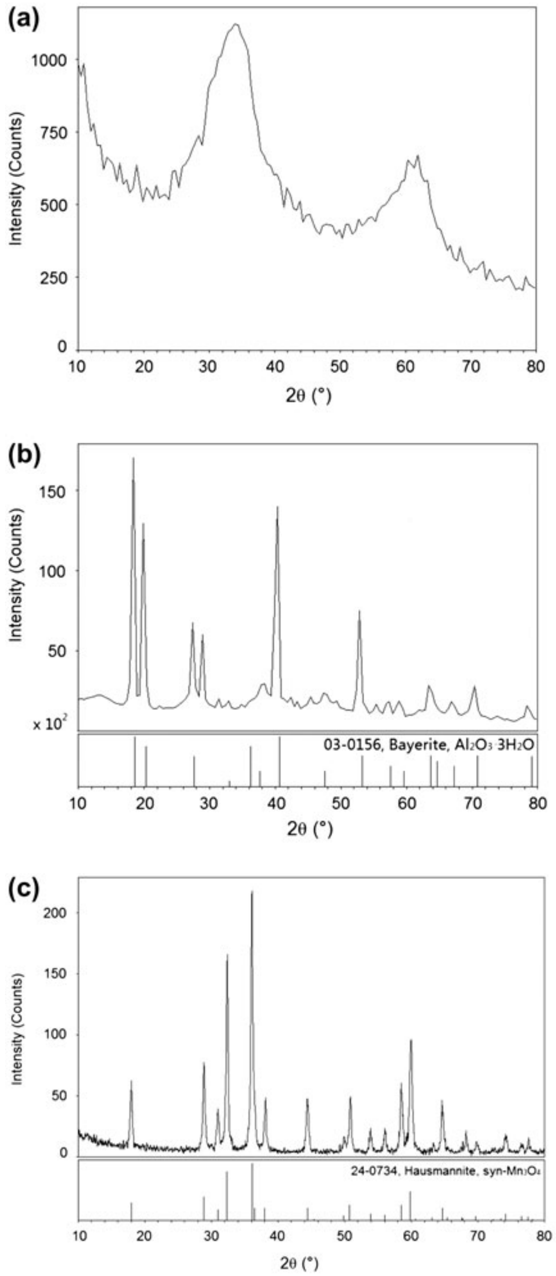

Fig. 1. XRD patterns of synthetic (a) ferrihydrite, (b) bayerite, and (c) hausmannite.

of various concentrations of ions (e.g. SO_4^{2-}, PO_4^{3-}, and Ca^{2+}) into the suspensions with an initial As(V) concentration of 0.4 mg L^{-1} (1.28 μM). The initial pHs of these suspensions with co-occurring ions were adjusted to 6.0 ± 0.1 by dilute HCl and NaOH. All suspensions were allowed to react, filter, and analysis as described above.

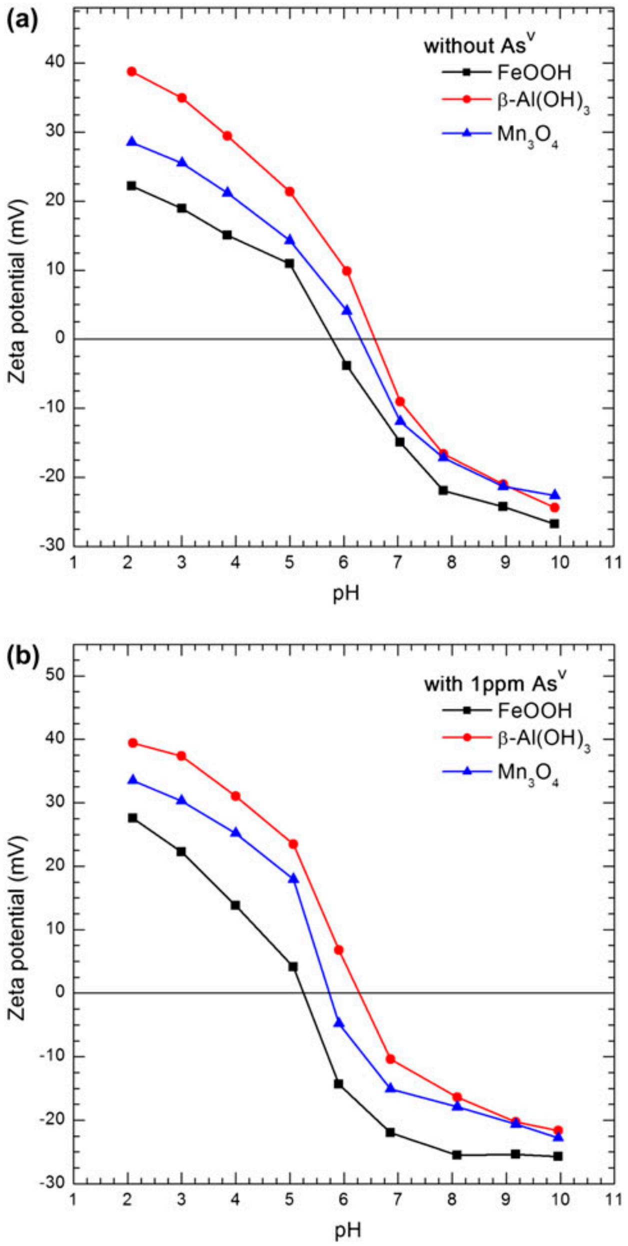

Fig. 2. Zeta potential (ζ) profiles of ferrihydrite (FeOOH), bayerite (β-$Al(OH)_3$), and hausmannite (Mn_3O_4) vs. pH in 0.1 M NaCl solution (a) without As(V) and (b) with 1 ppm (4.25 μM) As(V) at 298 ± 1 K.

2.4. Arsenate analysis

Arsenate analysis was measured on an AFS-200 atomic fluorescence spectrometer (AFS, Jiangsu Skyray Instrument Co., China) following the hydride-generation atomic fluorescence spectrometry (HG-AFS) procedure [28].

3. Results and discussion

3.1. Properties of Metal (oxyhydr)oxides

The synthetic metal (oxyhydr)oxides are 2-line ferrihydrite (FeOOH), bayerite (β-$Al(OH)_3$, JCPDS #03-0156), and hausmannite (Mn_3O_4, JCPDS #24-0734), respectively, as verified by XRD (Fig. 1). The two broad diffraction peaks centered at $2\theta \sim 34^\circ$ and 61° indicate that FeOOH was poorly crystallized (Fig. 1(a)) [2,29]. Both of the other two metal (oxyhydr)oxides were, however, well crystallized as indicated by their XRD patterns (Fig. 1(b) and (c)).

Fig. 2 shows the ζ profiles of FeOOH, β-$Al(OH)_3$, and Mn_3O_4 as a function of pH in 0.1 M NaCl solution. In the absence of As(V), FeOOH was negatively charged with pH increasing from 2 to 11, followed by Mn_3O_4 and β-$Al(OH)_3$. The point of zero charge (pH_{PZC}) of FeOOH, β-$Al(OH)_3$, and Mn_3O_4 are ~5.9, 6.7, and 6.3, respectively, in general accordance with previous studies [30,31]. However, in the presence of 1 mg L^{-1} As(V), the pH_{PZC} of all oxides shifted to more acidic, resulting in new pH_{PZC} values of ~5.2, 6.3, and 5.7, respectively. This was attributable to the strong complexation of As(V) onto the surface of these metal (oxyhydr)oxides, which can consequently shift the pH_{PZC} and ζ profiles [1,30,32,33].

3.2. Arsenate uptake envelopes

As shown in Fig. 3, the uptake envelopes of As(V) (initial [As(V)] = 4.0 mg L^{-1}) indicated that over 96% of As(V) was adsorbed by either FeOOH or β-$Al(OH)_3$ in pH 2–9, and ~95% of As(V) was sequestered by Mn_3O_4 in pH 2–8. The relatively strong adsorption of As(V) in the presence of 0.1 M NaCl suggests that As(V) complexed with these metal (oxyhydr)oxides to form an inner-sphere structure in pH 2–8 [25]. Comparison of these uptake envelopes indicated that As(V) adsorption began to decline above pH 6.5 for all adsorbents. This is attributed to the Coulombic repulsion between the negatively charged adsorbents and the As(V) species. At pH above 6.5, all adsorbents were negatively charged as indicated in the ζ profiles. Meanwhile, the dominant As(V) species would transform from $H_2AsO_4^-$ to $HAsO_4^{2-}$ with increasing pH above 6.5, leading to a further decrease in As(V) uptake [34–36].

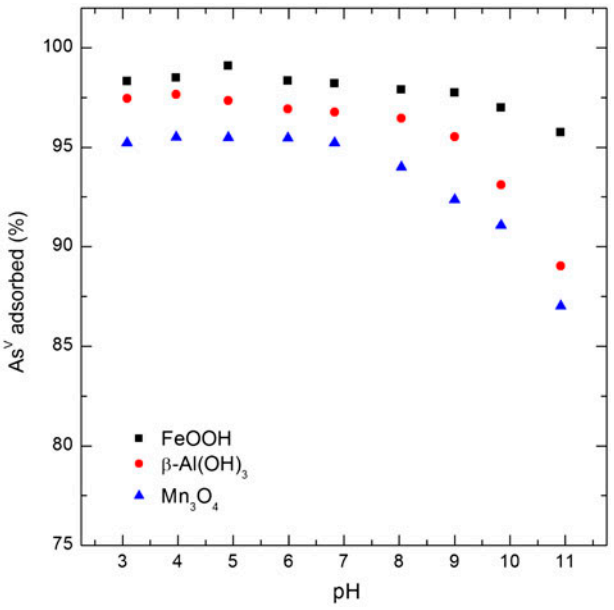

Fig. 3. Uptake envelopes of As(V) by ferrihydrite (FeOOH), bayerite (β-$Al(OH)_3$), and hausmannite (Mn_3O_4) in 0.1 M NaCl solution upon 24 h reaction at 298 ± 1 K (initial As(V): 0.4 mg L^{-1}, eq. 1.28 μM).

3.3. Arsenate equilibrium adsorption

The As(V) adsorption isotherms of three adsorbents are shown in Fig. 4. It was noted that all adsorption isotherms show a favorable type of adsorption, suggesting that As(V) was retained by strong complexation rather than by purely electrostatic adsorption [1]. As shown in Fig. 4, FeOOH shows a

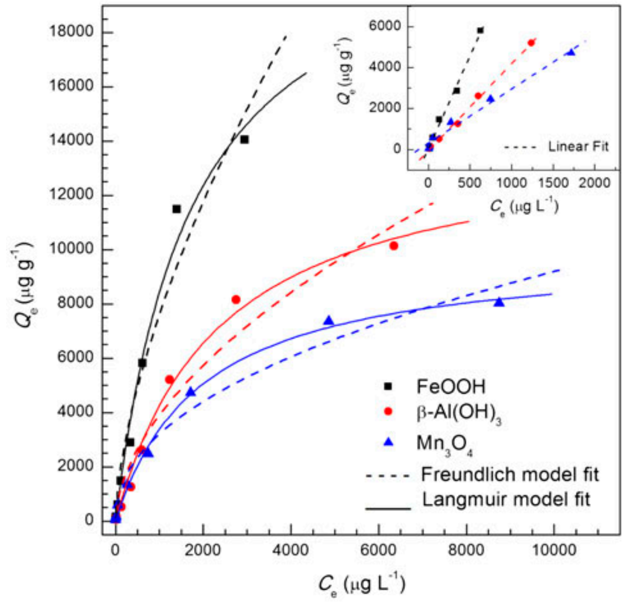

Fig. 4. Adsorption isotherms of As(V) by ferrihydrite (FeOOH), bayerite (β-$Al(OH)_3$), and hausmannite (Mn_3O_4) in 0.1 M NaCl at 298 ± 1 K. Inset is As(V) adsorption isotherms in the C_e (mg L^{-1}) rang of 0–2.00 and their linear fits.

much better performance in adsorption of As(V), followed by β-$Al(OH)_3$ and then Mn_3O_4. In general, the density of available adsorption sites plays a crucial role in As(V) uptake, i.e. lower As(V) uptake is believed to significantly attribute to the lower density of available adsorption sites of the adsorbents. It has shown that ferrihydrite has a very large surface area and a great amount of available adsorption sites, allowing it to be one of the most efficient adsorbents for aquatic As(V) [1,3,25,26,37]. However, the surface of β-$Al(OH)_3$ is relatively inert to adsorb As(V), because the two surface structural Al^{3+} are doubly coordinated by the OH^- groups at the crystal edges, reducing their availability of ligand exchange with other species [17,38]. Mn_3O_4 with the least As(V) adsorption capacity is believed to be the most stable state in all manganese oxides [39]; as a consequence, its surface is inactive for retaining As(V).

Both the Langmuir (Eq. (1)) and the Freundlich (Eq. (2)) equations were employed to fit the adsorption equilibrium data (Fig. 4), and the fitting parameters were obtained by nonlinear least-squares regression analysis and summarized in Table 1.

$$Q_e = \frac{Q_m C_e}{b + C_e} \tag{1}$$

$$Q_e = K_F C_e^{\frac{1}{n}} \tag{2}$$

where Q_e is the arsenic adsorption capacity, defined as the micrograms of arsenic removed at equilibrium per gram of adsorbents added (in mg As(V) g^{-1} adsorbent), C_e is the equilibrium arsenic concentration in mg L^{-1}, Q_m and b are the Langmuir fitting constants corresponding to the maximum adsorption capacity (MAC) (mg g^{-1}) and the binding constant (L mg^{-1}), respectively, and both K_F and n are Freundlich fitting constants. As shown in Table 1, all the correlation coefficients (R^2) calculated with the Langmuir equation are greater than those with the Freundlich equation, implying that the Langmuir model is better to fit the adsorption equilibrium data rather than the Freundlich model. All the n values are in the range of 1–10 (Table 1), which is a typical threshold showing that the As(V) adsorption are preferential processes and occurred spontaneously for all adsorbents [40]. The MAC of FeOOH, as calculated with the Langmuir equation, is 28.57 mg g^{-1} (91.56 μM g^{-1}), which is much greater than previously reported value of 2.66 mg g^{-1} for As(V) adsorption on hydrous ferric oxide (HFO) [3]. This discrepancy is probably attributed to the difference in the adsorbent/solution ratio, i.e. the ratio in our case is 33 times greater than that in the literature [3]. The calculated MACs of β-$Al(OH)_3$ and Mn_3O_4 are 14.29 mg g^{-1} and 1.00 mg g^{-1} (eq. 45.77 μM g^{-1} and 3.22 μM g^{-1}), respectively. It is reported that the fresh-made β-$Al(OH)_3$ have MACs of 991 μM g^{-1} and 702 μM g^{-1} for As(V) at pH 5 and 8, respectively [38], which are much greater than that in our case. The main reason for this lower MAC of β-$Al(OH)_3$, seems to derive from the drying process of the fresh-made β-$Al(OH)_3$ at 373 K, which consequently reduces the surface area and hence the amount of the available adsorption sites for As(V). Because hausmannite is one of the most unreactive manganese oxide species [41], the lower MAC for As(V) of synthetic hausmannite (Mn_3O_4) in the present study (i.e. 1.00 mg g^{-1}) would be reasonable from this perspective. To enhance the adsorption capacity for As(V), nanosized Mn_3O_4 (~25 nm) has been prepared and evaluated by Parsons et al. [42] However, the nanosized Mn_3O_4 showed a MAC of 212.0 μg g^{-1} for As(V) at the given pH, only one-fifth of the MAC in this study. Moreover, the stability and recovery of nanosized Mn_3O_4 remain to be challenging issues from a practical point of view.

It is noted that As(V) uptakes were linearly dependent on the equilibrium As(V) concentration (C_e) in the range of 0–2.0 mg L^{-1} for all adsorbents (see the inset of Fig. 4). This linear relationship may be useful in determination the optimum adsorbent/solution ratio with a known As(V) concentration [43]. Similar linear dependence had been observed in As(III)

Table 1
Fitting data of both the Langmuir and the Freundlich equations for adsorption of As(V) by FeOOH, β-$Al(OH)_3$, and Mn_3O_4 in 0.1 M NaCl at 298 ± 1 K (initial pH 6.0 ± 0.1)

	Langmuir			Freundlich		
Adsorbent	b (L mg^{-1})	Q_m (mg g^{-1})	R^2	K_F	n	R^2
FeOOH	2.14	28.57	0.989	99.23	1.59	0.956
β-$Al(OH)_3$	2.36	14.29	0.992	83.97	1.79	0.968
Mn_3O_4	0.20	1.00	0.995	136.61	2.18	0.976

adsorption on river sediments [4], and As(V) adsorption on Fe-based adsorbents systems [1,43].

All the adsorbents are particulate in shape, and hence probably cause hydraulic problems for the column-mode study of As(V) uptake. The column-mode study is widely adopted for practical operation and regeneration of the spent adsorbents for repeated utilization. However, it should be feasible and necessary to either embed the adsorbents to biopolymer gels [44,45] or load them onto porous supports [7–10] before the column-mode study in the future.

3.4. Arsenate adsorption kinetics

Adsorption kinetics experiments ($C_0 = 0.67\ \text{mg L}^{-1}$) were performed in 0.1 M NaCl solutions with pH 6.1 ± 0.1 and the results were presented in Fig. 5. In each case, the remaining As(V) concentration decreased rapidly in the first 2 h and then declined gradually over the next 8 h. These processes are the typical rapid adsorption—slow adsorption process. The duration of either rapid or slow adsorption processes is dependent on many factors, including pH, the initial As(V) concentration, the affinity of the adsorbents, the surface area of the adsorbents, the adsorbent/solution ratio, etc. For example, with an adsorbent/solution ratio of $2\ \text{g L}^{-1}$, the rapid adsorption process achieved in the first 0.5 h has been observed for As(V) adsorption by FeOOH at pH 9.2 [25]. It is also reported that the fresh ferrihydrite (FeOOH) with high surface area has a rapid adsorption of 5 min toward As(V) [11]. Aging of fresh ferrihydrite would reduce its surface area and eventually affect the rapid adsorption kinetic [37]. When using ferrihydrite aged at 313 K for 4 h as adsorbent for As(V), it shows that the rapid adsorption of As(V) lasted for 2 h in this study, which confirms the previous observation [11,37]. Rapid adsorption of As(V) by nanosized Mn_3O_4 in 5 min was also observed [42], which is much faster than the Mn_3O_4 adsorbent (~2 h) used here.

The adsorption kinetic data were fitted with the pseudo-second-order kinetic equations as listed in Eqs. (3) and (4) [46]:

$$Q_t = \frac{k_2 Q_e^2 t}{k_2 Q_e t + 1} \tag{3}$$

$$\frac{t}{Q_t} = \frac{1}{k_2 Q_e^2} + \frac{1}{Q_e} t \tag{4}$$

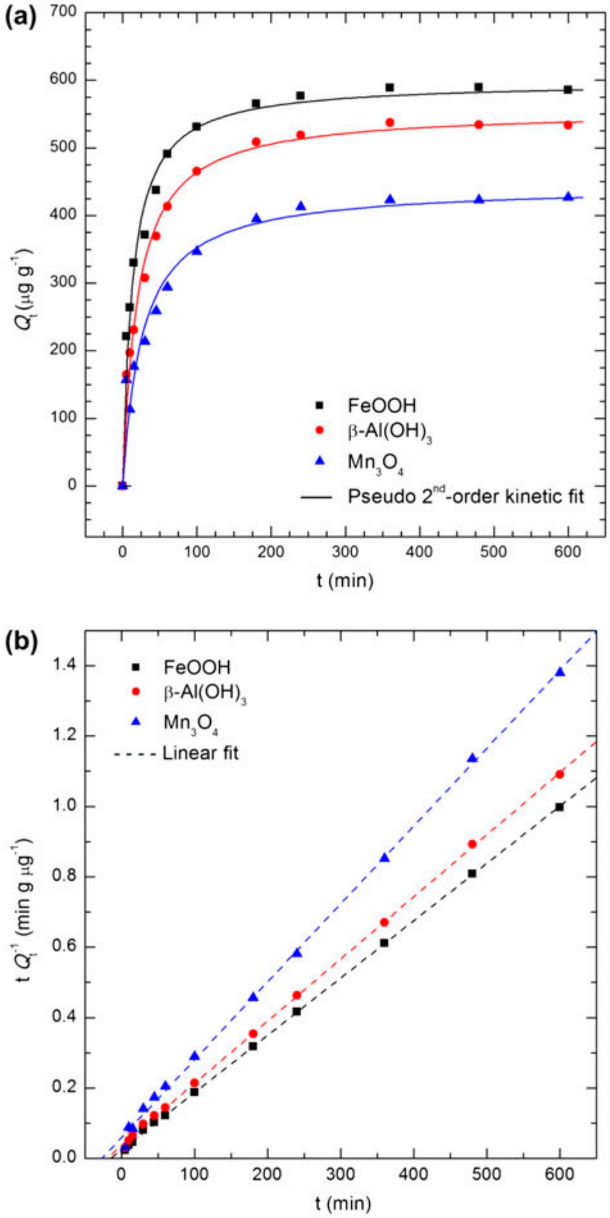

Fig. 5. Kinetic curves of As(V) adsorption by ferrihydrite (FeOOH), bayerite (β-$Al(OH)_3$), and hausmannite (Mn_3O_4) in 0.1 M NaCl at 298 ± 1 K. (a) $Q_t \sim t$; (b) $t\ Q_t^{-1} \sim t$ (initial [As(V)]: $0.67\ \text{mg L}^{-1}$, eq. 8.84 μM). All initial pH values were adjusted to 6.0 ± 0.1 with dilute HCl and NaOH.

where Q_e is the equilibrium adsorption capacity in mg g^{-1}, Q_t (mg g^{-1}) is the adsorption capacity at time t, and t is contacting time in min, k_2 is the pseudo-second-order rate constant in $\text{g mg}^{-1}\ \text{min}^{-1}$. Q_t was calculated by $Q_t = (C_0 - C_t) \times V/M$, where C_0 is the initial As(V) concentration in mg L^{-1}, C_t is the As(V) concentration at time t, V is the volume of the suspension in mL, and M is the mass of adsorbent added (g). Fig. 5(b) shows the plots of $t\ Q_t^{-1}$ vs. t to determine $Q_{e.c.}$ as well as the correlation coefficient values (R^2) of

Table 2
Fitting parameters from the pseudo-second-order rate equation for adsorption of As(V) by FeOOH, β-Al(OH)$_3$, and Mn$_3$O$_4$ in 0.1 M NaCl at 298 ± 1 K (initial pH 6.0 ± 0.1)

	Fitting parameters from pseudo-second-order kinetic model			
Adsorbent	k_2 (g mg^{-1} min^{-1})	$Q_{t\,=\,10\,\text{h}}$ (mg g^{-1})	$Q_{\text{e.c.}}$ (mg g^{-1})	R^2
FeOOH	0.129	0.59	0.60	0.987
β-Al(OH)$_3$	0.091	0.54	0.56	0.991
Mn$_3$O$_4$	0.085	0.43	0.45	0.989

these adsorbents. The fitting parameters were summarized in Table 2. The correlation coefficients (R^2) of all adsorbents are greater than 0.98, indicating that the pseudo-second-order kinetic model can well fit all kinetic data. The adsorption capacities at 10 h reaction ($Q_{t\,=\,10\,\text{h}}$) were almost equal to the calculated values ($Q_{\text{e.c.}}$), implying that the adsorption equilibrium may reach over 10 h. In fact, the adsorption equilibrium of As(V) by ferrihydrite could be achieved within 4 h [1]. However, it is also shown that As(V) can continue to

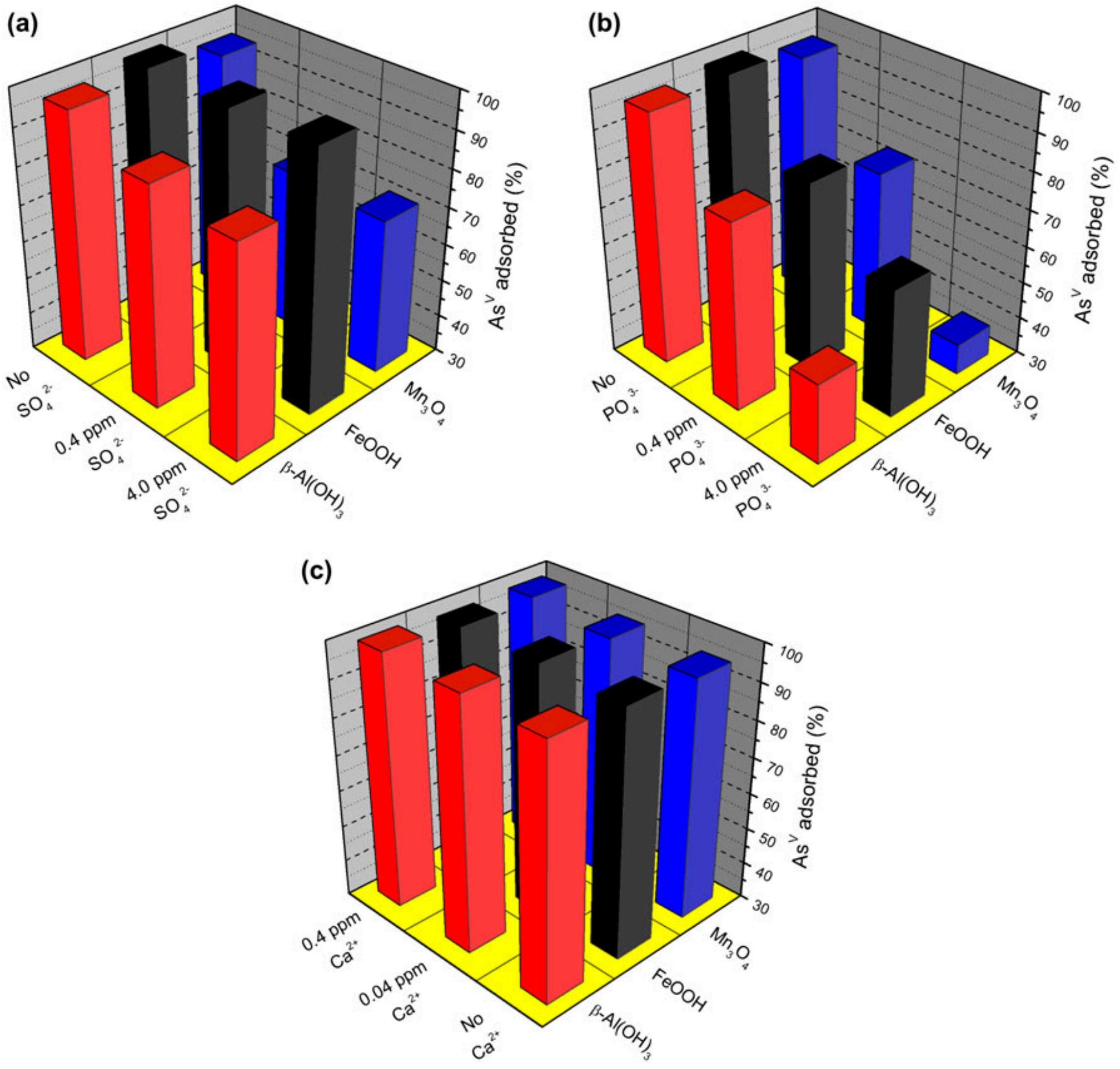

Fig. 6. Effect of SO_4^{2-} (a), PO_4^{3-} (b), and Ca^{2+} (c) on As(V) adsorption in 0.1 M NaCl at 298 ± 1 K.

be adsorbed onto the post-synthetic ferrihydrite for several days after an initial rapid adsorption [11]. In this study, we supposed the adsorption equilibrium could be obtained within 24 h; therefore, all adsorption equilibrium experiments were conducted with a reaction time of 24 h.

3.5. Competitive adsorption for As(V)

Competitive adsorption from co-occurring oxoanions or counterions can play a crucial role in As(V) uptake by metal minerals when considering the natural aquatic systems. Both phosphate (PO_4^{3-}) and sulfate (SO_4^{2-}) are typical competitive oxyanions to As(V) because their molecular structures are analogous to that of arsenate anion [18,47,48]. Whereas co-occurring calcium ion (Ca^{2+}) can enhance the As(V) uptake on HFO by adhesion to the surface of HFO, resulting in a positive surface that is favorable for adsorption of As (V) anions [12].

In As(V) uptake with an initial concentration of 0.40 mg L^{-1} (1.28 μM), addition of sulfate was observed to decrease As(V) uptake by either β-$Al(OH)_3$ or Mn_3O_4, whereas did not affect As(V) uptake on FeOOH even increasing [SO_4^{2-}] up to 4.0 mg L^{-1} (Fig. 6(a)). This independence of As(V) uptake by ferrihydrite upon the presence of sulfate has also been reported previously [12,49]. When further increasing [SO_4^{2-}] to 4.0 mg L^{-1}, the adsorption efficiencies of either β-Al$(OH)_3$ or Mn_3O_4 only decreased slightly (Fig. 6(a)). This phenomenon indicated that both β-$Al(OH)_3$ and Mn_3O_4 probably have two different kinds of active sites with different affinity to As(V) and sulfate, respectively [50,51]. Similar co-occurrence of two different kinds of active sites for different anions has been reported for other metal (hydr)oxides [34,50–52]. On the other hand, the addition of phosphate with final [PO_4^{3-}] of 4.0 mg L^{-1} to the adsorption systems consequently led to a drop of As(V) adsorption efficiencies by 55, 44, and 35% for FeOOH, β-$Al(OH)_3$, and Mn_3O_4, respectively, as compared to that without phosphate (Fig. 6(b)). This is comparable with previous reports [48,49]. As for calcium ions, the addition of Ca^{2+} yielded an enhanced As(V) uptake for all adsorbents (Fig. 6(c)), which was contributed from the shift of pH_{PZC} of all adsorbents to more alkaline by the adhesion of Ca^{2+} to their surfaces [12], forming more positive surfaces that are favorable for As(V) uptake. However, further spectroscopy-based structural evidences may be necessary to clarify the real contributions of Ca^{2+} at the molecular level.

4. Conclusions

In the present study, the equilibrium and kinetics of As(V) adsorption by three metal (oxyhydr)oxides, i.e. ferrihydrite (FeOOH), bayerite (β-$Al(OH)_3$), and hausmannite (Mn_3O_4), have been investigated. Equilibrium studies implied that As(V) uptake by all adsorbents follows the Langmuir model rather than the Freundlich model. The MACs calculated with the Langmuir equation are 28.57, 14.29, and 1.00 mg g^{-1} for FeOOH, β-$Al(OH)_3$, and Mn_3O_4, respectively. Kinetic studies suggest that all As(V) adsorption kinetic data can be well fitted with the pseudo-second-order rate model with correlation coefficients (R^2) greater than 0.98. Furthermore, co-occurring adsorbates, such as sulfate and phosphate, are found to reduce the As(V) uptake, whereas calcium ion can enhance the As(V) adsorption for all adsorbents. Our findings will clarify the conflicting conclusions of the equilibrium and the kinetics models in previous reports and extend the understanding the equilibrium and kinetic behaviors of As(V) adsorption by metal (oxyhydr)oxides under the same conditions.

Acknowledgments

The work was financially supported by NSFC (grant numbers. 51002080, 5130105009), CSC (grant number 2011832032), the Priority Academic Program Development of Jiangsu Higher Education Institutions and Collaborative Innovation Center of Atmospheric Environment and Equipment Technology. Jing Wang and Dongyang Nie are grateful for their experimental assistance.

References

[1] M.L. Pierce, C.B. Moore, Adsorption of arsenite and arsenate on amorphous iron hydroxide, Water Res. 16 (1982) 1247–1253.
[2] L. Carlson, J.M. Bigham, U. Schwertmann, A. Kyek, F. Wagner, Scavenging of as from acid mine drainage by schwertmannite and ferrihydrite: A comparison with synthetic analogues, Environ. Sci. Technol. 36 (2002) 1712–1719.
[3] S. Dixit, J.G. Hering, Comparison of arsenic(V) and arsenic(III) sorption onto iron oxide minerals: Implications for arsenic mobility, Environ. Sci. Technol. 37 (2003) 4182–4189.
[4] T.R. Holm, M.A. Anderson, D.G. Iverson, R.S. Stanforth, Heterogeneous interactions of arsenic in aquatic systems, in: Chemical Modeling in Aqueous Systems, American Chemical Society, Washington, DC, 1979, pp. 711–736.
[5] D. Mohan, C.U. Pittman, Arsenic removal from water/wastewater using adsorbents—A critical review, J. Hazard. Mater. 142 (2007) 1–53.

[6] T. Hiemstra, W.H. Van Riemsdijk, Surface structural ion adsorption modeling of competitive binding of oxyanions by metal (hydr)oxides, J. Colloid Interface Sci. 210 (1999) 182–193.

[7] L. Cumbal, A.K. Sengupta, Arsenic removal using polymer-supported hydrated iron(III) oxide nanoparticles: Role of donnan membrane effect, Environ. Sci. Technol. 39 (2005) 6508–6515.

[8] M.R. Awual, S.A. El-Safty, A. Jyo, Removal of trace arsenic(V) and phosphate from water by a highly selective ligand exchange adsorbent, J. Environ. Sci. 23 (2011) 1947–1954.

[9] M.R. Awual, A. Jyo, Rapid column-mode removal of arsenate from water by crosslinked poly(allylamine) resin, Water Res. 43 (2009) 1229–1236.

[10] M.R. Awual, S. Urata, A. Jyo, M. Tamada, A. Katakai, Arsenate removal from water by a weak-base anion exchange fibrous adsorbent, Water Res. 42 (2008) 689–696.

[11] C.C. Fuller, J.A. Davis, G.A. Waychunas, Surface chemistry of ferrihydrite: Part 2. Kinetics of arsenate adsorption and coprecipitation, Geochim. Cosmochim. Acta 57 (1993) 2271–2282.

[12] J.A. Wilkie, J.G. Hering, Adsorption of arsenic onto hydrous ferric oxide: Effects of adsorbate/adsorbent ratios and co-occurring solutes, Colloids Surf., A 107 (1996) 97–110.

[13] F.H. Li, H. Fu, J.P. Zhai, Q. Li, Synthesis of mesostructured ferric oxyhydroxides templated by alkyl surfactants: Effect of pH, F- and solvents, and their adsorption isotherms for As(V), Microporous Mesoporous Mater. 123 (2009) 177–184.

[14] M. Kanematsu, T.M. Young, K. Fukushi, P.G. Green, J.L. Darby, Individual and combined effects of water quality and empty bed contact time on As(V) removal by a fixed-bed iron oxide adsorber: Implication for silicate precoating, Water Res. 46 (2012) 5061–5070.

[15] W. Li, R. Harrington, Y.Z. Tang, J.D. Kubicki, M. Aryanpour, R.J. Reeder, J.B. Parise, B.L. Phillips, Differential pair distribution function study of the structure of arsenate adsorbed on nanocrystalline γ-alumina, Environ. Sci. Technol. 45 (2011) 9687–9692.

[16] Y. Arai, E.J. Elzinga, D.L. Sparks, X-ray absorption spectroscopic investigation of arsenite and arsenate adsorption at the aluminum oxide-water interface, J. Colloid Interface Sci. 235 (2001) 80–88.

[17] P.M. Huang, M.K. Wang, N. Kämpf, D.G. Schulze, Aluminum hydroxides, in: Soil Mineralogy with Environmental Applications, SSSA Book Series 7, Madison, WI, 2002, pp. 261–289.

[18] E.W. Shin, J.S. Han, M. Jang, S.H. Min, J.K. Park, R.M. Rowell, Phosphate adsorption on aluminum-impregnated mesoporous silicates: Surface structure and behavior of adsorbents, Environ. Sci. Technol. 38 (2004) 912–917.

[19] V.Q. Chiu, J.G. Hering, Arsenic adsorption and oxidation at manganite surfaces. 1. Method for simultaneous determination of adsorbed and dissolved arsenic species, Environ. Sci. Technol. 34 (2000) 2029–2034.

[20] G.C. Silva, F.S. Almeida, A.M. Ferreira, V.S.T. Ciminelli, Preparation and application of a magnetic composite (Mn_3O_4/Fe_3O_4) for removal of As(III) from aqueous solutions, Mater. Res.-Ibero-Am. J. 15 (2012) 403–408.

[21] G.C. Silva, F.S. Almeida, M.S.S. Dantas, A.M. Ferreira, V.S.T. Ciminelli, Raman and IR spectroscopic investigation of As adsorbed on Mn_3O_4 magnetic composites, Spectrochim. Acta, Part A 100 (2013) 161–165.

[22] B.A. Manning, S. Goldberg, Modeling competitive adsorption of arsenate with phosphate and molybdate on oxide minerals, Soil Sci. Soc. Am. J. 60 (1996) 121–131.

[23] B.A. Manning, S.E. Fendorf, B. Bostick, D.L. Suarez, Arsenic(III) oxidation and arsenic(V) adsorption reactions on synthetic birnessite, Environ. Sci. Technol. 36 (2002) 976–981.

[24] W. Driehaus, R. Seith, M. Jekel, Oxidation of arsenate (III) with manganese oxides in water-treatment, Water Res. 29 (1995) 297–305.

[25] K.P. Raven, A. Jain, R.H. Loeppert, Arsenite and arsenate adsorption on ferrihydrite: Kinetics, equilibrium, and adsorption envelopes, Environ. Sci. Technol. 32 (1998) 344–349.

[26] P.J. Swedlund, J.G. Webster, Adsorption and polymerisation of silicic acid on ferrihydrite, and its effect on arsenic adsorption, Water Res. 33 (1999) 3413–3422.

[27] F.H. Li, Layer-by-layer loading iron onto mesoporous silica surfaces: Synthesis, characterization and application for As(V) removal, Microporous Mesoporous Mater. 171 (2013) 139–146.

[28] J.B. Shi, Z.Y. Tang, Z.X. Jin, Q. Chi, B. He, G.B. Jiang, Determination of As(III) and As(V) in soils using sequential extraction combined with flow injection hydride generation atomic fluorescence detection, Anal. Chim. Acta 477 (2003) 139–147.

[29] Y.F. Jia, D.N. Zhang, R.R. Pan, L.Y. Xu, G.P. Demopoulos, A novel two-step coprecipitation process using Fe(III) and Al(III) for the removal and immobilization of arsenate from acidic aqueous solution, Water Res. 46 (2012) 500–508.

[30] W. Wainipee, D.J. Weiss, M.A. Sephton, B.J. Coles, C. Unsworth, R. Court, The effect of crude oil on arsenate adsorption on goethite, Water Res. 44 (2010) 5673–5683.

[31] C.M. Su, D.L. Suarez, In situ infrared speciation of adsorbed carbonate on aluminum and iron oxides, Clays Clay Miner. 45 (1997) 814–825.

[32] J.J. Lenhart, B.D. Honeyman, Uranium(VI) sorption to hematite in the presence of humic acid, Geochim. Cosmochim. Acta 63 (1999) 2891–2901.

[33] C.A.J. Appelo, M.J.J. Van der Weiden, C. Tournassat, L. Charlet, Surface complexation of ferrous iron and carbonate on ferrihydrite and the mobilization of arsenic, Environ. Sci. Technol. 36 (2002) 3096–3103.

[34] Y.T. Liu, M.K. Wang, T.Y. Chen, P.N. Chiang, P.M. Huang, J.F. Lee, Arsenate sorption on lithium/aluminum layered double hydroxide intercalated by chloride and on gibbsite: Sorption isotherms, envelopes, and spectroscopic studies, Environ. Sci. Technol. 40 (2006) 7784–7789.

[35] B.A. Manning, S. Goldberg, Modeling arsenate competitive adsorption on kaolinite, montmorillonite and illite, Clays Clay Miner. 44 (1996) 609–623.

[36] M.J. DeMarco, A.K. Sengupta, J.E. Greenleaf, Arsenic removal using a polymeric/inorganic hybrid sorbent, Water Res. 37 (2003) 164–176.

[37] G.A. Waychunas, B.A. Rea, C.C. Fuller, J.A. Davis, Surface chemistry of ferrihydrite: Part 1. EXAFS studies of the geometry of coprecipitated and adsorbed arsenate, Geochim. Cosmochim. Acta 57 (1993) 2251–2269.

[38] Y. Masue, R.H. Loeppert, T.A. Kramer, Arsenate and arsenite adsorption and desorption behavior on coprecipitated aluminum: Iron hydroxides, Environ. Sci. Technol. 41 (2007) 837–842.

[39] W.X. Zhang, Z.H. Yang, Y. Liu, S.P. Tang, X.Z. Han, M. Chen, Controlled synthesis of Mn_3O_4 nanocrystallites and MnOOH nanorods by a solvothermal method, J. Cryst. Growth 263 (2004) 394–399.

[40] G. McKay, H.S. Blair, J.R. Gardner, Adsorption of dyes on chitin. I. Equilibrium studies, J. Appl. Polym. Sci. 27 (1982) 3043–3057.

[41] R.M. McKenzie, The synthesis of birnessite, cryptomelane, and some other oxides and hydroxides of manganese, Mineral. Mag. 38 (1971) 493–502.

[42] J.G. Parsons, M.L. Lopez, J.R. Peralta-Videa, J.L. Gardea-Torresdey, Determination of arsenic(III) and arsenic(V) binding to microwave assisted hydrothermal synthetically prepared Fe_3O_4, Mn_3O_4, and $MnFe_2O_4$ nanoadsorbents, Microchem. J. 91 (2009) 100–106.

[43] J.L. Mathieu, A.J. Gadgil, S.E.A. Addy, K. Kowolik, Arsenic remediation of drinking water using iron-oxide coated coal bottom ash, J. Environ. Sci. Health Part A-Toxic/Hazard. Subst. Environ. Eng. 45 (2010) 1446–1460.

[44] J.H. Min, J.G. Hering, Arsenate sorption by Fe(III)-doped alginate gels, Water Res. 32 (1998) 1544–1552.

[45] S.M. Miller, M.L. Spaulding, J.B. Zimmerman, Optimization of capacity and kinetics for a novel bio-based arsenic sorbent, TiO_2-impregnated chitosan bead, Water Res. 45 (2011) 5745–5754.

[46] Y.S. Ho, G. McKay, Sorption of dye from aqueous solution by peat, Chem. Eng. J. 70 (1998) 115–124.

[47] Y. Gao, A. Mucci, Individual and competitive adsorption of phosphate and arsenate on goethite in artificial seawater, Chem. Geol. 199 (2003) 91–109.

[48] A. Jain, R.H. Loeppert, Effect of competing anions on the adsorption of arsenate and arsenite by ferrihydrite, J. Environ. Qual. 29 (2000) 1422–1430.

[49] D. Hawke, P.D. Carpenter, K.A. Hunter, Competitive adsorption of phosphate on goethite in marine electrolytes, Environ. Sci. Technol. 23 (1989) 187–191.

[50] Y. Kiso, Y.J. Jung, T. Yamada, M. Nagai, K.S. Min, Removal properties of arsenic compounds with synthetic hydrotalcite compounds, in: J. Clement, S. Parsons (Eds.), Leading-Edge Technology 2005—Water Treatment, IWA Publishing, London, 2005, pp. 75–81.

[51] Y. Zhang, X.M. Dou, M. Yang, H. He, C.Y. Jing, Z.Y. Wu, Removal of arsenate from water by using an Fe–Ce oxide adsorbent: Effects of coexistent fluoride and phosphate, J. Hazard. Mater. 179 (2010) 208–214.

[52] R. Chitrakar, S. Tezuka, A. Sonoda, K. Sakane, K. Ooi, T. Hirotsu, Adsorption of phosphate from seawater on calcined MgMn-layered double hydroxides, J. Colloid Interface Sci. 290 (2005) 45–51.